Journal of Chromatography B, 879 (2011) 1043–1048

Contents lists available at ScienceDirect

Journal of Chromatography B

journal homepage: www.elsevier.com/locate/chromb

A novel matrix derivatized from hydrophilic gigaporous polystyrene-based microspheres for high-speed immobilized-metal affinity chromatography

Jian-Bo Qu[a,*], Yong-Dong Huang[b], Guang-Lun Jing[a], Jian-Guo Liu[a], Wei-Qing Zhou[b], Hu Zhu[a,*], Jian-Ren Lu[a]

[a] Center for Bioengineering and Biotechnology, China University of Petroleum (East China), QingDao 266555, PR China
[b] National Key Laboratory of Biochemical Engineering, Institute of Process Engineering, Chinese Academy of Sciences, Beijing 100190, PR China

ARTICLE INFO

Article history:
Received 26 November 2010
Accepted 4 March 2011
Available online 12 March 2011

Keywords:
Gigaporous
Polystyrene microspheres
Column efficiency
Immobilized-metal affinity chromatography
Superoxide dismutase

ABSTRACT

Agarose coated gigaporous polystyrene microspheres were evaluated as a novel matrix for immobilized-metal affinity chromatography (IMAC). With four steps, nickel ions were successfully immobilized on the microspheres. The gigaporous structure and chromatographic properties of IMAC medium were characterized. A column packed with the matrix showed low column backpressure and high column efficiency at high flow velocity. Furthermore, this matrix was used for purifying superoxide dismutase (SOD), which was expressed in *Escherichia coli* (*E. coli*) in submerged fermentation, on an Äkta purifier 100 system under different flow velocities. The purity of the SOD from this one-step purification was 79% and the recovery yield was about 89.6% under the superficial flow velocity of 3251 cm/h. In conclusion, all the results suggested that the gigaporous matrix has considerable advantages for high-speed immobilized-metal affinity chromatography.

1. Introduction

Immobilized-metal affinity chromatography (IMAC) is one of the most powerful techniques in selective purification and isolation of various proteins, making use of coordinative binding of some amino acid residues exposed on the surface [1]. Though the numbers of surface accessible histidines ultimately limits the application of immobilized metal affinity to only a few natural proteins, engineering of a high affinity for chelated metal ions into a specific protein makes that recombinant protein unique [2], and thereby easy to isolate from its contaminants. IMAC was first introduced by Everson and Parker [3], who applied immobilized chelating compounds to purify metalloproteins. As pseudo affinity ligands for affinity separations, chelated metal ions offer many advantages over classical biological affinity types, such as ligand stability, high capacity, mild elution conditions, simple regeneration and low cost [4]. These factors are important when large-scale purification procedures are involved.

Success of IMAC depends on many factors. The property of matrix is one of the most important factors. Classical stationary phases are based on the polysaccharide soft gels, such as cellulose, dextran and agarose. While polysaccharides are biocompatible and can be easily activated, they exhibit poor mechanical strength and only can be operated under low pressure [5], which limits their use in large-scale industry. On the other hand, inorganic supports, mainly silica, have excellent mechanical properties, but suffer from poor chemical stability and high non-specific adsorption [6]. To overcome the disadvantages of polysaccharides and inorganic materials, synthesized polymer resins have been widely studied as alternatives since the late 1970s. Organic resins usually possess mechanical strength orders of magnitude greater than soft gels and can tolerate extreme environmental conditions, such as pH1 and pH12. However, for conventional porous microspheres, slow mass transfer rate is the limiting factor that restricts their application in biomacromolecules separation [6]. In 1990s, a novel polystyrene (PS) based medium, i.e. POROS perfusion absorbent, was introduced to reduce the problem of stagnant mobile phase mass transfer [7]. POROS microspheres were prepared by nanomicrosphere agglomeration method, which have two sets of pores, through pores (600–800 nm) and diffusive pores (80–150 nm). The interconnected through pores bring intraparticle convective transport into the bead and diffusive pores provide a substantial surface area. As a result, a POROS matrix can be operated at high speed while maintaining high column efficiency and dynamic binding capacity [6–10]. Nevertheless, the POROS medium suffers from a complicated preparation method and high cost, and there are few recent reports about the application of POROS. Inspired by HIPE (high internal phase emulsion) method [11,12], Ma et al. [13] have developed a novel surfactant reverse micelles swelling method to prepare gigaporous PS microspheres with pore size

* Corresponding author. Fax: +86 532 86981566.
E-mail addresses: jbqu@upc.edu.cn (J.-B. Qu), huzhu@upc.edu.cn (H. Zhu).

1570-0232/$ – see front matter © 2011 Elsevier B.V. All rights reserved.
doi:10.1016/j.jchromb.2011.03.015

of *ca.* 300–500 nm, which overcomes the preparation problem of POROS medium described above and can be used as perfusion chromatographic supports. Unfortunately, the native PS beads possess low biocompatibility due to their high hydrophobicity, which leads to non-specific adsorption and denaturation of proteins. In a previous study, we have successfully modified the gigaporous PS microspheres with agarose derivative [14], which makes the surface of the particles rich in hydroxyl groups and biocompatible. The hydrophilic gigaporous PS microspheres are good chromatographic base supports for different types of chromatography since the coatings can be easily activated by classical methods.

SOD plays an important role in defending against superoxide anion toxicity, radioactive risk and preventing aging as it can eliminate oxygen free radicals in the body [15]. It is one of the most important metalloenzymes for aerobic and anaerobic organisms, which constitute the first line of defense against oxidative stress [16]. It has been found that the activity of SOD is related to some diseases, such as tumor and inflammation [17]. It is therefore of importance to develop a quick, economic and easy to scale-up purification procedure for industrial application of SOD.

In this paper, with agarose coated gigaporous PS (Agap-co-PS) microspheres as a base support [14], we have prepared iminodiacetic acid (IDA)–Ni (II) metal chelator medium (APS–Ni) and evaluated its affinity chromatographic behavior. The gigaporous IMAC matrix was also applied in one-step purification of thermostable SOD with 6 histidine tags, which was expressed in *E. coli*.

2. Experimental

2.1. Materials

The Agap-co-PS microspheres used in this study were prepared in our previous study [14]. The coating amount was 81.97 mg/g dry microspheres, the specific surface area was 24.09 m^2/g, the average diameter was 55 μm (30–85 μm range), and the average pore size was 300 nm (100–500 nm range). The Agap-co-PS microspheres were stored in 20% (v/v) ethanol–water solution at room temperature for further process.

Bovine serum albumin (BSA, Mw 67,000), Imidazole (AR) and ethylenediamine tetraacetic acid (EDTA, AR) were all ordered from Sigma (St. Louis, MO, USA); Isopropyl β-D-1-thiogalactopyranoside (IPTG, dioxane free) was from Promega (Madison, USA); Protein marker (14.4–94.0 kDa) was purchased from Beijing Tiangen Biotech Co., Ltd. (China); Allyl glycidyl ether (AR) was obtained from Shanghai Bangcheng Chemical Co., Ltd. (China); Bromine water (3 wt%), iminodiacetic acid (IDA, AR), Nickel nitrate (AR) and murexide (AR) were from Sinopharm Chemical Reagent Co. Ltd. (China); Restriction enzyme and polymerase were from TaKaRa (Dalian, China). Primer synthesis and DNA sequencing were done in Sangon (Shanghai, China); Kits and other reagents used in molecular manipulations were obtained from Intron Company (China). Other reagents were all of analytical grade from local sources.

2.2. Feedstock preparation

The superoxide dismutase from *T. thermophilus* HB27 (Accession: AB010884) was cloned into pET-28a $^{(+)}$ to obtain the recombinant pETSOD, which was transformed into competent cell *E. coli* BL21 (DE3). Expression of the SOD was performed according to the pET system manual (Novagen, Germany). Since the SOD was manganese-containing protein [18], manganese ion was supplemented (as $MnCl_2$) at initial concentration of 2 mM with IPTG (0.01 mM) to start the induced expression. Expression was optimized to be 8 h at 37 °C with orbital shaker at 250 rpm. The cells were harvested by centrifugation at 4612 × *g* (Sigma 6-16 K, Germany) for 15 min at 4 °C.

The pelleted cells were resuspended in phosphate-buffered saline (PBS) buffer (pH 7.4) three times to wash the residue of fermentation broth on the cells. Finally, the cell suspension was cracked with ultrasonication (Bilon92-II, Shanghai Bilon Instruments Co., LTD.) at 400 W for 2 s with 2 s intervals in an ice bath for duration of 99 times. The suspension was centrifuged at 4612 × *g* for 15 min at 4 °C. The clarified supernatant, i.e., crude enzyme solution, was used as feedstock for the subsequent IMAC purification process.

2.3. Preparation of chelator medium (APS–Ni)

The gigaporous chelator microspheres were prepared by four-step reaction. Briefly, the Agap-co-PS microspheres were first introduced double bond through allyl group activation, then the allyl-activated microspheres were reacted with bromine water to introduce bromo group. Iminodiacetic acid (IDA) was next coupled onto brominated gigaporous PS microspheres through a nucleophilic substitution reaction. At last nickel ions were chelated on the particles coupled with IDA. Further preparation details can be found in Supplementary data.

2.4. Characterization of APS–Ni

The pore structure of gigaporous PS microspheres before and after derivatization was observed by scanning electron microscopy (SEM, Hitachi S-4800, Japan). Mercury porosimetry measurements (MPM) were conducted by an AutoPore IV 9500 mercury porosimetry (Micromeritics, USA) to study the difference between APS–Ni and PS microspheres. Hydrated density of wet microspheres was measured with a 25 ml pycnometer.

The gigaporous PS and APS–Ni microspheres were respectively packed into stainless steel columns (100 mm × 4.6 mm I.D.) by slurry packing method on an Äkta purifier 100 system (GE Healthcare), and all the chromatographic experiments were conducted on the same system. The mechanical stability and permeability of medium was evaluated through the effect of flow rate on the back pressure of column with high-purity water as mobile phase. In addition, the bed permeability (*K*) can be evaluated by the Darcy's law in a laminar flow region [19].

$$K = \frac{\mu u L}{\Delta P} \quad (1)$$

where μ is the viscosity of the mobile phase (Pa s), u the superficial velocity (cm/s), L the length of column (cm), and ΔP the column pressure-drop (Pa).

The amount of chelated ions on particles was detected with the following method. The microspheres were packed into a glass column (20 cm × 1 cm I.D.) and washed with deionized water thoroughly, then, 10 CVs of 0.05 mol/l standard nickel nitrate solution was used to elute the column and the eluate was collected. Afterwards, the column was further washed with deionized water to remove unbound ions on APS–Ni and the eluate was collected too. Combined these two eluates and adjusted the pH to 8.0 by adding ammonia. Finally, using murexide as indicator, the nickel ions in the eluate were titrated with 0.1 mol/l EDTA solution until the color of solution changing from yellow to purple. The amount of chelated ions was determined by the mass balance of nickel ions and the same volume of fresh nickel nitrate solution was used as control.

2.5. Chromatography

The column efficiency was evaluated in terms of HETP (the height equivalent to a theoretical plate). The experiments were

conducted at flow velocities ranging from 180 to 2528 cm/h under a non-retained condition. The mobile phase was 20 mM sodium phosphate, 500 mM NaCl, 500 mM imidazole, pH 7.4 and BSA was used as a probe protein. After equilibrating the column with 10 CVs of mobile phase, 200 μl of protein sample was injected and the chromatogram was recorded at the column exit with a UV detector at 280 nm. The dead volume of the system was measured by injecting 200 μl of 20% (v/v) acetone solution via the injection loop.

2.6. Purification of SOD from crude enzyme with APS–Ni column

To investigate the high-speed chromatographic separation performance of APS–Ni column, 100 μl of feedstock was loaded into the equilibrated column under different flow velocities followed by washing. Equilibration, feed application and washing were performed with 20 mM sodium phosphate, 500 mM NaCl, 100 mM imidazole, pH 7.4 (buffer A). After washing the column with 3 CVs of buffer A to remove impurity, 5 CVs of elution buffer containing 20 mM sodium phosphate, 500 mM NaCl, 500 mM imidazole, pH 7.4 (buffer B) was used to elute the bound SOD from the matrix with step gradient at room temperature.

2.7. Characterization of purified SOD

2.7.1. SOD activity analysis

The activity of SOD was measured with a modified procedure of pyrogallol autooxidation [20]. One unit of SOD activity is defined as the amount of enzyme required to inhibit the autooxidation rate of pyrogallol to 50%. The recovery of SOD was calculated from the following equation.

$$\text{SOD recovery}\,(\%) = \frac{\text{total activity of product solution}}{\text{total activity of crude solution}} \times 100\% \quad (2)$$

2.7.2. SOD molecular weight measurement

Gel filtration chromatography is a method for separating proteins and peptides based on their size. From this point, we can estimate the molecular weight (Mw) of SOD with a calibration curve of the column. In this study, the eluate peak of IMAC and crude enzyme were analyzed using Äkta purifier 100 system equipped with a size exclusion chromatography column Superose 6 10/300 GL (Tricorn, GE Healthcare, Sweden). The mobile phase was 50 mM sodium phosphate, pH 7.0 and the flow velocity was fixed at 0.4 ml/min. After equilibrating the column with 10 CVs of mobile phase, 100 μl of sample protein was injected via the injection loop. The protein concentration was monitored at 280 nm and calibration curves obtained with proteins of known Mw (Log Mw versus retention volume) were used to determine the Mw of SOD.

2.7.3. SOD purity analysis

By using gel filtration chromatography, the purity of SOD separated from IMAC was evaluated by the following equation.

$$\text{SOD purity}\,(\%) = \frac{\text{peak area of SOD}}{\text{total peak area}} \times 100\% \quad (3)$$

The purity of the eluted peak under different flow velocities from crude enzyme solution was also analyzed by sodium dodecyl sulfate–polyacrylamide gel electrophoresis (SDS–PAGE). The SDS–PAGE analysis was performed on 12 wt% gels using a DYY-6 C electrophoresis system (LiuYi Apparatus Factory, Beijing, China) with a Tanon VE-180 electrophoresis cell (gel size: 8.2 cm × 8.2 cm). Detection of the protein bands was performed with the Coomassie Brilliant Blue R-250 staining method. The gel image was acquired on Tanon-1600 gel image system (Tanon, Shanghai, China).

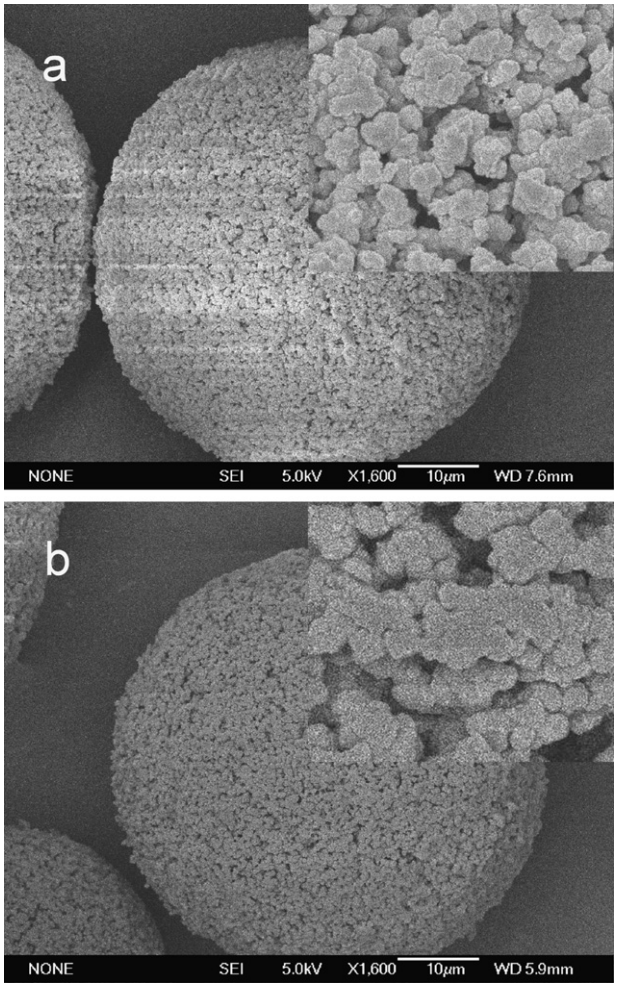

Fig. 1. SEM images of gigaporous PS (a, 1600×; inset, 9000×) microspheres and APS–Ni (b, 1600×; inset, 9000×).

3. Results and discussion

3.1. Physical properties of the matrix

Fig. 1 shows the SEM images of gigaporous PS microspheres and APS–Ni. After hydrophilic coating and functional derivatization, little change on the pore morphology was observed, and the gigaporous structure was well maintained. In addition, some highly reticular gigapores larger than 500 nm could be observed in the inset to Fig. 1. Fig. S1 also confirmed the gigapores of particles remained relatively unchanged after coating and functionalization (see Supplementary data). These gigapores in APS–Ni are highly promising in providing an interconnected path for convective flow in chromatography.

Fig. 2 shows the effect of flow velocity on the back pressure of PS and APS–Ni column. The results show a linear relationship for both columns with flow velocity up to 3612 cm/h. This indicates that the microspheres had good mechanical stability and no microspheres were broken up after derivatization. Moreover, the back pressure of PS and APS–Ni column under 3612 cm/h was only 0.28 MPa and 0.35 MPa, respectively. Many factors such as particle pore structure, shape, size, swelling degree and compatibility with mobile phase can change the back pressure of column. However, these factors except for pore structure may contribute negligibly to low back

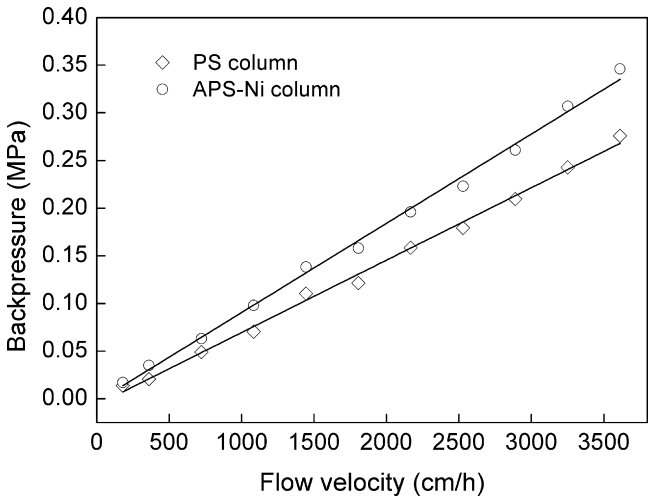

Fig. 2. Relationship between the column back pressure and flow velocity. Column, 100 mm × 4.6 mm I.D.; mobile phase, high-purity water.

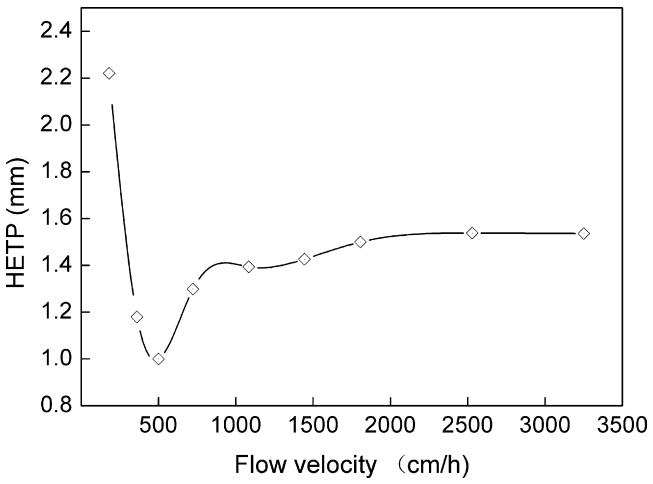

Fig. 3. Column efficiency versus flow velocity. Column, 100 mm × 4.6 mm I.D.; sample, 2 mg/ml BSA; mobile phase, 20 mM sodium phosphate, 500 mM NaCl, 500 mM imidazole, pH 7.4.

pressure of column in our study. Because the average particle size of PS microspheres is only 55 μm, and the swelling degree is negligible when the mobile phase, high purity water, is poor solvent to PS. The low back pressure of columns is an evidence for the presence of flow-through pores, which reduce the flow resistance. The same phenomenon has been reported with other macroporous beads [21,22]. In previous study [14], we have confirmed that mobile phase in the column flowed not only through the spaces between matrix but also through the gigapores of particles, i.e. the existence of through pores in gigaporous microspheres. According to experimental data, the bed permeability (K) can be calculated from Eq. (1), and the value of K for both columns is higher than that for conventional columns we reported earlier [23] (see Table 1). This further confirmed the good permeability of gigaporous particles. It can also be seen from Fig. 2 that the back pressure of APS–Ni column increased slightly. This was probably because the pore size of the microspheres decreased slightly after coating and functionalization.

The physical properties of gigaporous PS microspheres and APS–Ni are listed in Table 1. After hydrophilic coating (Agap-co-PS) and functionalization, the water content of APS–Ni is evidently higher than that of native PS particles, which is advantageous for decreasing non-specific adsorption of biomacromolecules on the matrix. The amount of chelated ions on particles could be controlled in the range of 10–120 μmol/ml medium according to practical requirements. In this study the optimized amount of chelated ions on particles was 40.5 μmol/ml medium.

3.2. Column efficiency

HETP is a typical criterion to describe the overall column efficiency. In this paper, BSA was used as a probe and the HETP was measured under the non-retained condition. Fig. 3 shows the relationship between HETP and flow velocity for the APS–Ni column. HETP exhibited a typical curve defined by the Van Deemter equation when the flow velocity was lower than 500 cm/h, which indicated that the longitudinal diffusion occupies dominant effect in this regime. When the flow velocity was higher than 500 cm/h, however, the HETP of APS–Ni column only increased slightly with flow velocity up to 3250 cm/h, i.e. HETP was nearly independent of flow velocity in a wide range of flow rate. This is opposite to conventional porous medium columns, the HETPs of which strongly depend on flow velocity [21,22]. We speculate that the presence of flow-through pores in APS–Ni particles may induce intraparticle convective mass transfer for BSA and significantly reduce the stagnant mobile phase mass transfer of particles by reducing the diffusive distance [8].

Table 1
Physical properties of PS and APS–Ni particles.

Particle	ρ_w (mg/ml)	Water content (wt%)	Immobilized ions capacity (μmol/ml medium)	K (m^2) × 10^{10}
PS	1.01	19.41	–	3.52
APS–Ni	1.03	62.76	40.5	2.71

3.3. Purification of SOD from fermentation broth

In order to further verify the advantages of APS–Ni column in high-speed IMAC, SOD from *E. coli* feedstock was purified on an APS–Ni column under different flow velocities. The chromatograms obtained are shown in Fig. 4. The results show that the APS–Ni column could purify SOD within 2 min at velocity up to 3251 cm/h, which is very promising for high-speed IMAC. Owing to the absorbance of imidazole at 280 nm, the UV baseline did not return its initial level.

The collected SOD fraction and feedstock were analyzed using Äkta purifier 100 system equipped with a Superose 6 10/300 GL column (Fig. 5). It can be seen that there were six peaks in the crude enzyme solution. After purification, the SOD sample had only one major peak at an elution volume of 16.27 ml. This indicates that the purity of SOD was effectively improved after passing through APS–Ni column.

The SOD purification fold, recovery and purity under different flow velocities are listed in Table 2. As listed in Table 2, the SOD purification fold, recovery and purity only decreased slightly with flow velocity up to 3251 cm/h. The average purification fold, SOD recovery and purity were 16.4, 95.6% and 84% respectively. At a flow velocity of 3251 cm/h, the SOD recovery and purity could still reach 89.6% and 79% respectively. The chromatograms and purified data of SOD further confirmed the existence of gigapores in particles can improve mobile phase mass transfer rate.

3.4. Electrophoresis

The SOD purified on APS–Ni column at different flow velocities were analyzed with SDS–PAGE. As the electrophoretogram

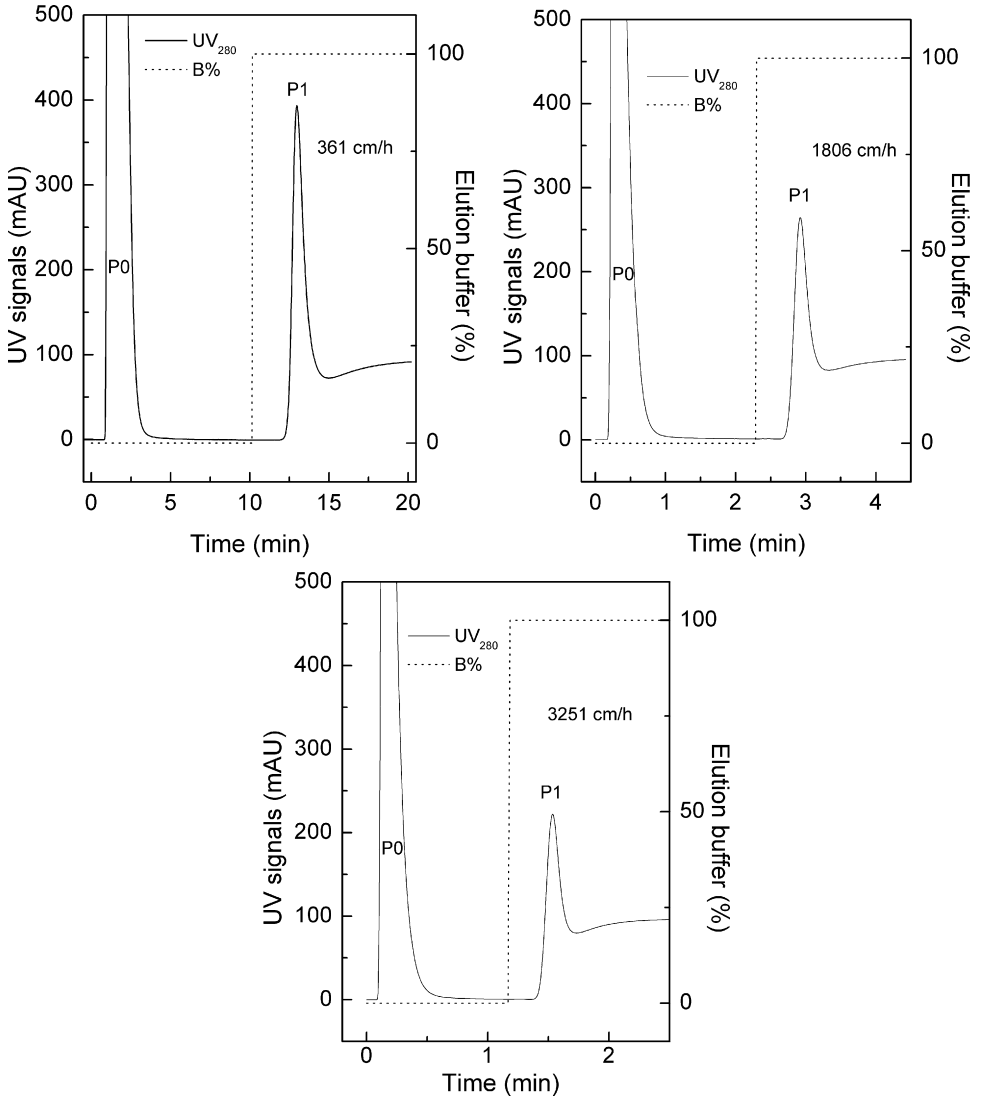

Fig. 4. Chromatograms of SOD on APS–Ni column under different flow velocities. Column, 100 mm × 4.6 mm i.d.; 20 mM sodium phosphate, 500 mM NaCl, 100 mM imidazole, pH 7.4; injection size, 100 μl; step gradient, 100% buffer A to 100% buffer B after washing step; P0, breakthrough peak; P1, elution peak.

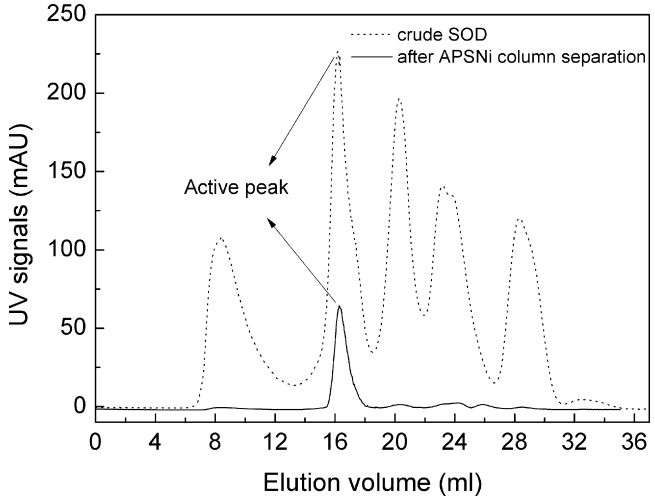

Fig. 5. Comparison of gel filtration chromatograms at 280 nm using a Superose 6 10/300 GL column. Dot, crude enzyme solution; solid, SOD sample purified by APS–Ni column under flow velocity of 361 cm/h.

in Fig. 6 shows, all the purified SOD samples exhibit one major band near 24 kDa, which is consistent with the primary band in the feedstock. The molecular weight of SOD estimated by an Äkta purifier 100 system on Superose 6 10/300 GL column was around 100 kDa, suggesting that the native SOD is a tetramer.

Table 2
The purification of SOD from clarified feedstock at different flow velocity using APS–Ni column.

Flow velocity (cm/h)	Purification fold	SOD recovery (%)	SOD purity (%)
361	18.3	100	88
722	16.6	100	87
1084	18.0	100	86
1806	15.9	94.1	83
2528	15.2	89.8	80
3251	14.6	89.6	79
Average	16.4	95.6	84

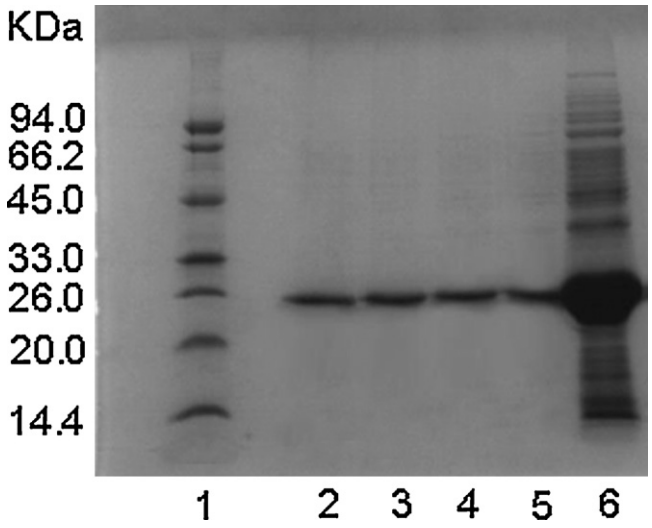

Fig. 6. SDS–PAGE analysis of SOD samples purified from crude enzyme solution under different flow velocities. Lanes: 1, molecular weight marker; 2, 3, 4 and 5 is SOD sample purified under flow velocities of 361, 1084, 1806 and 2528 cm/h, respectively; 6, feedstock.

4. Conclusions

A novel IMAC matrix for high-speed protein chromatography has been prepared by using hydrophilic gigaporous Agap-co-PS microspheres as a base support. The gigaporous structure of APS–Ni medium was characterized with pore size analysis and SEM images. The low back pressure of an APS–Ni column revealed the presence of flow-through pores in the gigaporous medium. Accelerated mass transfer induced by convective flow of mobile phase through the gigapores in the medium was demonstrated by its high column efficiency and high protein resolution at high flow velocity. The excellent recovery and high purity of the SOD after purification on APS–Ni column suggest that the IMAC matrix is well suitable for the quick separation of recombinant proteins with histidine tags. All the results support that the gigaporous matrix has good potential for high-speed preparative protein chromatography.

Acknowledgements

We would like to thank the Fundamental Research Funds for the Central Universities, the Natural Science Foundation of Shandong Province (no. ZR2010BM001) and the Doctoral Foundation of Shandong Province (no. 2008BS02018).

Appendix A. Supplementary data

Supplementary data associated with this article can be found, in the online version, at doi:10.1016/j.jchromb.2011.03.015.

References

[1] V. Gaberc-Porekar, V. Menart, J. Biochem. Biophys. Methods 49 (2001) 335.
[2] F.H. Arnold, Bio/Technology 9 (1991) 150.
[3] R.J. Everson, H.E. Parker, Bioinorg. Chem. 4 (1974) 15.
[4] F.C. Chong, W.S. Tan, D.R. Awang Biak, T.C. Ling, B.T. Tey, J. Chromatogr. B 877 (2009) 1561.
[5] L.E. Weaver Jr., G. Carta, Biotechnol. Progr. 12 (1996) 342.
[6] N.B. Afeyan, N.F. Gordon, L. Mazasaroff, L. Varady, S.P. Fulton, Y.B. Yang, F.E. Regnier, J. Chromatogr. 519 (1990) 1.
[7] N.B. Afeyan, F.E. Regnier, R.C. Dean, 1991. US Patent No. 5,019,270.
[8] N.B. Afeyan, S.P. Fulton, F.E. Regnier, J. Chromatogr. 544 (1991) 267.
[9] M. McCoy, K. Kalghatgi, F.E. Regnier, N.B. Afeyan, J. Chromatogr. A 743 (1996) 221.
[10] D. Whitney, M. McCoy, N. Gordon, N.B. Afeyan, J. Chromatogr. A 807 (1998) 165.
[11] D. Barby, Z. Haq, 1985. US Patent No. 4,522,953.
[12] N.H. Li, J.R. Benson, N. Kitagawa, 2000. US Patent No. 6,100,306.
[13] W.Q. Zhou, T.Y. Gu, Z.G. Su, G.H. Ma, Polymer 48 (2007) 1981.
[14] J.B. Qu, W.Q. Zhou, W. Wei, Z.G. Su, G.H. Ma, Langmuir 24 (2008) 13646.
[15] C.L. Yao, A.L. Wang, W.N. Wang, R.Y. Sun, Aquaculture 341 (2004) 621.
[16] A.R. Reddi, L.T. Jensen, A. Naranuntarat, L. Rosenfeld, Free Radical Biol. Med. 46 (2009) 154.
[17] J.S. Kroll, P.R. Langford, K.E. Wilks, A.D. Keil, Microbiology 141 (1995) 2271.
[18] T.W. Wang, A.D. Qiu, F.G. Meng, H.M. Zhou, Mol. Biotechnol. 42 (2009) 146.
[19] R.M. De la vega, C. Chenou, J.M. Loureiro, A.E. Rodrigue, Biochem. Eng. J. 1 (1998) 11.
[20] H.Z. Gu, L.Q. Lu, Q.S. Yuan, J. Zhao, Chin. Pharm. Biotechnol. 13 (2006) 377.
[21] G.Y. Sun, Q.H. Shi, Y. Sun, J. Chromatogr. A 1061 (2004) 159.
[22] Y. Shi, Y. Sun, Chromatographia 57 (2003) 29.
[23] J.B. Qu, X.Z. Wan, Y.Q. Zhai, W.Q. Zhou, Z.G. Su, G.H. Ma, J. Chromatogr. A 1216 (2009) 6511.